



Hydrogel Metal Nanoparticles Composites For Biomedical Application

Jaafar Abdullah Omar, Mohammed Khalil Younis

Department of Chemistry, College of Science, University of Zakho, Zakho, Iraq

Corresponding author E-mail: jaafar.omer@staff.uoz.edu.krd

<http://dx.doi.org/10.13005/ojc/420122>

(Received: May 15, 2025; Accepted: August 12, 2025)

ABSTRACT

Producing chitosan beads hydrogel with antimicrobial properties is the purpose of this research. First, Chitosan has been dissolved in diluted ethanoic acid to create a uniform solution. Different concentrations of myrrh gum were prepared in distilled water, followed by the addition of sodium hydroxide and silver nitrate. The chitosan solution was then carefully added to mixture myrrh, sodium hydroxide and silver nitrate to produce hydrogel silver nanoparticles beads. After this step, beads were cleaned and dried for characterization. Swelling test has been done in three different pH values (4,7 and 10). FTIR analysis revealed that some bands were shifted in wavelength of composite chitosan, myrrh, and silver species. These shifts indicated that an interaction happened in the new composite. XRD analysis verified the presence of the chitosan phase and showed a decrease in crystallinity with addition of silver nitrate and a change myrrh concentration, which means a significant alteration occurred within the structure of the produced beads. There has been an alteration to the inside of the structure. FESEM revealed a noticeable shift in morphology, going from smooth to rougher and more uneven. The antibacterial efficacy was evaluated for different concentrations of hydrogel in acidic solution to determine minimum concentration of composite to inhibit the bacterial growth.

keywords: Hydrogel, Myrrh, chitosan, sodium hydroxide, nanoparticles, silver nitrate.

INTRODUCTION

Hydrogels are a category of flexible material that can be made originates from either natural or man-made entities. They are very important in the fields of biomedicine, of particular importance in the fields of tissue science, medicines that are administered in a regulated manner and regenerative medicine [1],[2],[3],[4],[5],[6],[7],[8],[9],[10],[11]. This is important because their physical, chemical, and biological properties are very similar to biological tissues [12],[13],[14],[15]. The exoskeletons of insects and crustaceans contain chitin, a naturally occurring biodegradable material that may be also synthesized by deacetylating of chitin [16]. Its versatile nature stems from the fact that its reactive

amino and hydroxyl functional groups are readily modifiable, opening up several potential applications. [17]. One of its main features is that it works as an antibacterial agent when it comes into contact with microbial cell membranes in acidic environments [18]. However, its practical value is diminished by its limited solubility in neutral and alkaline conditions [19]. Hydrogels derived from chitosan are widely used in medicine because they are safe for living things and breaks down naturally. It's used for medicine, healing wounds, and growing new tissue. [20]. Studies show that combining chitosan with other materials, including magnetic nanoparticles, makes it stronger and more effective for several medical uses [21]. Myrrh substance comes from plants in the



Commiphora family. Its composition includes a blend of gums, oils, and resins. The resin fraction contains a lot of bioactive parts, like commiphoric acids, sterols, and triterpenoids[22]. Chemically, Myrrh is classified as oleo-gum resin. Water soluble part components of myrrh are polysaccharides, proteins, and oxidase enzymes make up the bulk of the gum component, which accounts for about 40% to 60%. The rest of the myrrh part component (20% to 40%) are dissolved in alcohol[23],[24]. Silver nanoparticles (AgNPs) has been strong antibacterial action against several infectious and harmful microbes, including drug-resistant species[25][26]. In conclusion, the aim of this work is to produce hydrogel silver nanoparticles beads, measuring its swelling degree and its antibacterial efficiency.

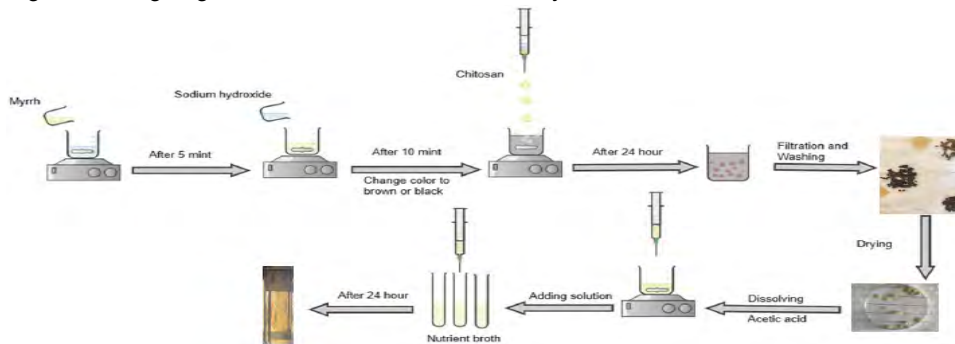


Figure 1. Graphical Abstract Fabrication of Chitosan–Myrrh–Silver Hydrogel Beads For Antibacterial Purposes

MATERIALS AND METHODS

Materials

Chitosan, sodium hydroxide and silver nitrate are provided by Molekula. Myrrh from a local market. Nutrient broth and Acetic acid from Sigma-Aldrich. Deionized water and D.W were utilized for all preparations.

Preparation of hydrogel

Chitosan solution was made by dissolving in diluted acetic acid solution with continues stirring until the solution was homogenous. Different concentration from water soluble portion of myrrh were prepared. To create the hydrogel, a beaker was filled with an appropriate volume of sodium hydroxide solution, then myrrh solution was added to the mixture in ten minutes with continues stirring. After that, the silver nitrate solution was added, and the mixture was stirred for five minutes. The clear solution becomes brownish or black which indicates the producing of nanoparticles. After that chitosan has been added dropwise to produce hydrogel silver nanoparticles beads.

Characterizations

Swelling analysis of prepared hydrogel beads. Three distinct pH settings were used to examine the swelling, and the swelling percentage

was determined using the gravimetric technique.

Fourier Transform Infrared Spectroscopy (FTIR)

FTIR spectroscopy was applied to analyze the chemical structure of chitosan, myrrh and the synthesized chitosan–myrrh–silver hydrogel. FTIR spectra of pure chitosan (A), chitosan with sodium hydroxide (B), chitosan with sodium hydroxide and myrrh (C), and chitosan with sodium hydroxide, myrrh, and silver nitrate (D). The Perkin-Elmer 1710-FTIR spectrometer was used to get IR spectra at the University of Mosul.

X-ray diffraction (XRD)

The X-ray diffraction pattern (XRD) of four chosen samples: chitosan figure (E), chitosan combined with myrrh and sodium hydroxide figure (F), and chitosan combined with myrrh, sodium hydroxide, and silver nitrate figure (H). X-ray diffraction (XRD) investigation was conducted using a DX-2700BH diffractometer with Cu K radiation ($\lambda = 0.154 \text{ nm}$) throughout a 2θ range of $5\text{--}80^\circ$. Field Emission Scanning Electron Microscopy (FESEM)

The FESEM is used to analysis the beads' morphology of the hydrogel. Pure chitosan figure (L), chitosan with myrrh and sodium hydroxide figure (M) and chitosan with myrrh, sodium

hydroxide and silver nitrate figure (N). The dried beads were put on stubs that had a thin layer of gold on them, and then they were photographed with a (FE-SEM, JSM-7600F, JEOL, Japan).

Biological activity

The broth dilution technique has been used to determine the minimal concentration of an antibiotic solution that inhibits the growth of bacteria. To achieve this, a series of diluted samples of the antibacterial agent in nutrient broth were prepared, followed by the addition of the bacterial culture solution to each sample. The minimal inhibitory concentration (MIC) was determined to be this value.

RESULTS AND DISCUSSION

Swelling studies

The swelling behavior of the chitosan samples was clearly influenced by both pH and composition. Chitosan that had been treated with sodium hydroxide exhibit limited swelling. The highest swelling was observed at pH 10, while the lowest swelling happened at pH 4 and was even lower at pH 7. After adding myrrh, the swelling went up at all pH levels, which means that myrrh makes the polymer network more open and able to take in water. The swelling was lower at pH 10 than at pH 4, and it was worse at pH 7 than at pH 4. At pH 4 and pH 7, myrrh and silver nitrate samples swelled the most. This means that they have a structure that is very porous and rich in ions, which makes them very water-attracting. On the other hand, swelling went down a lot when the pH went up to 10. This was probably because there were less chitosan protonation and the network got tighter. Overall, the results demonstrate that the swelling capacity of chitosan-based materials is strongly affected by both pH and the presence of additional composite. Therefore, the produced hydrogel could be classified as pH-respond hydrogel.

Fourier Transform Infrared Spectroscopy (FTIR)

The presence of a wide band at 3288 cm^{-1} , a band at 1589 cm^{-1} , and a prominent fingerprint area around $1150\text{--}1025\text{ cm}^{-1}$ all support the idea that this the spectrum of pure chitosan (Fig A) [27]. A more prominent band at 1670 cm^{-1} (amide I, C=O) appears after sodium hydroxide solution treatment, in addition to a minor change at 1069 cm^{-1} and bands at $901, 686, 635,$ and 557 cm^{-1} . Deprotonation

and interactions between sodium and chitosan are responsible for these structural alterations (Fig B). An ester in myrrh leads to new peaks at 1732 cm^{-1} . Chitosan primary amine and conjugated C=C from myrrh are detected at 1652 cm^{-1} in the chitosan-myrrh system, whereas secondary amine (II/N-H) bending with potential aromatic contributions and CH/COO vibrations are at 1584 cm^{-1} and $1435\text{--}1360\text{ cm}^{-1}$, respectively. (Fig C) shows that these peaks indicate the presence of neutralized or deprotonated groups in the matrix. The addition of silver nitrate causes the amide band to shift from 1652 to 1645 cm^{-1} . The bands at $597, 518,$ and 420 cm^{-1} indicate that vibrations involving Ag-O/metal-oxygen are taking place, whereas the shifts at $1584, 1260, 1149, 1059,$ and 1020 cm^{-1} demonstrate that Ag is coordinating (Fig D).

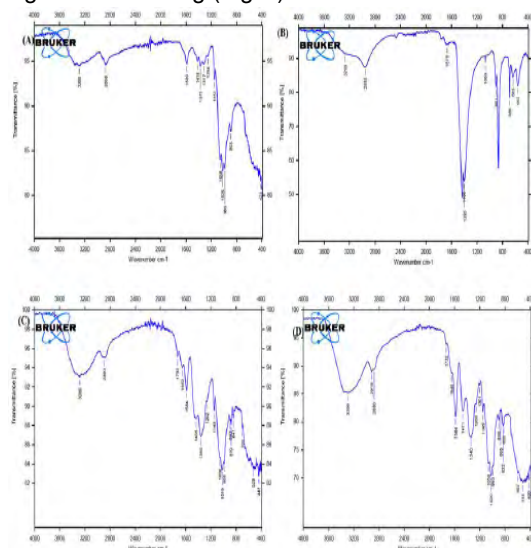


Figure 2. FTIR spectra of (A) pure chitosan, (B) chitosan treated with sodium hydroxide, (C) chitosan treated with sodium hydroxide and myrrh, (D)

X-RD Diffraction

The XRD data reveals that the structural phases vary between samples, and it is evident that crystallinity varies as a function of sample type. The appearance of pure chitosan is like the usual chitosan polymer phase. There is a high degree of crystallinity (97.68%) and a broad diffraction peak (around 20°) because hydrogen bonds hold the molecules in the chains together as shown in figure (E). The chitosan peak at 20° is still present after adding myrrh and sodium hydroxide, but there are now more distinct reflections. Secondary crystalline phases are observed, as shown here. These are

probably sodium-containing ionic or crystalline domains created in an alkaline environment, or crystalline components associated with myrrh. At the same time, crystallinity slightly decreases, indicating that the chitosan is mostly undigested as shown in figure (F). The diffractogram still displays the chitosan phase with increasing amounts of AgNO₃, but now it also includes reflections from silver-containing crystalline phases. As a result, the silver was properly incorporated. Even more reduction occurs in crystallinity, reaching 87.22%. This implies that the composite is less organized because silver species disrupt the chitosan chain, which is the most important bond shown in figure (H).

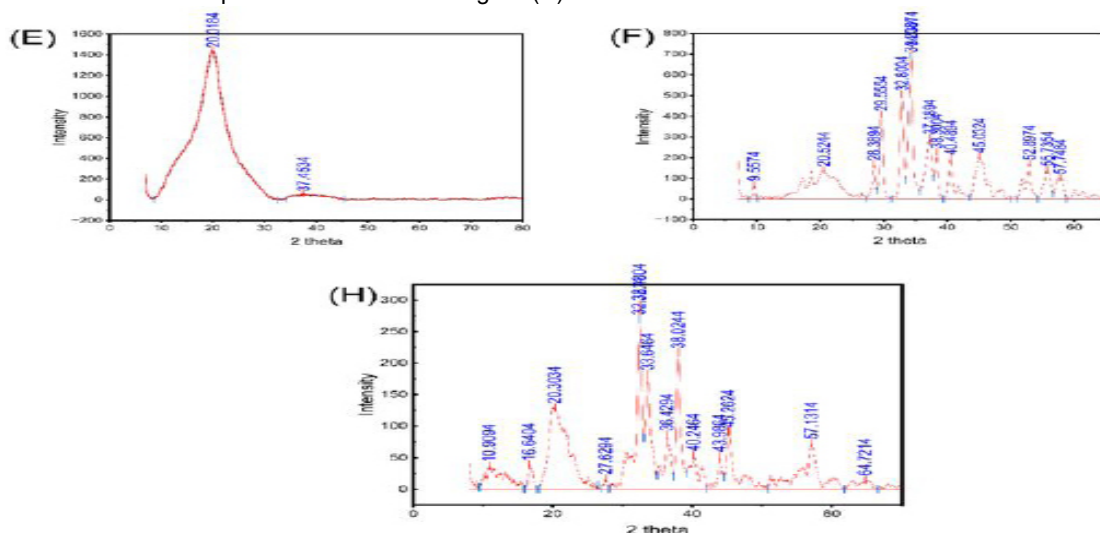


Figure 3. XRD pattern of (E) pure chitosan, (F) chitosan treated with sodium hydroxide and myrrh, (H) The composite of chitosan, myrrh, NaOH, and AgNO₃.

Field Emission Scanning Electron Microscopy (FTESM)

The pure form of chitosan appears as an extremely rough, thin sheet. Shrinkage has created microcracks in the matrix, which also possesses small granular and multilayer characteristics, as shown in figure (L). The chitosan surface becomes much rougher and less even after adding myrrh and sodium hydroxide. The structure changes to layers of folded areas covered in tightly packed nodules that come together to form larger clusters. This makes the surface appear more porous and generates tiny spaces between them, as seen in figure (M). After adding silver nitrate, the surface becomes even rougher and new bright particles appear on the chitosan–myrrh matrix, which appear as rods or plates with small groups on them in the higher-modification image. As a result, rather than forming a homogeneous polymer structure, silver forms distinct loaded domains on the surface figure (N).

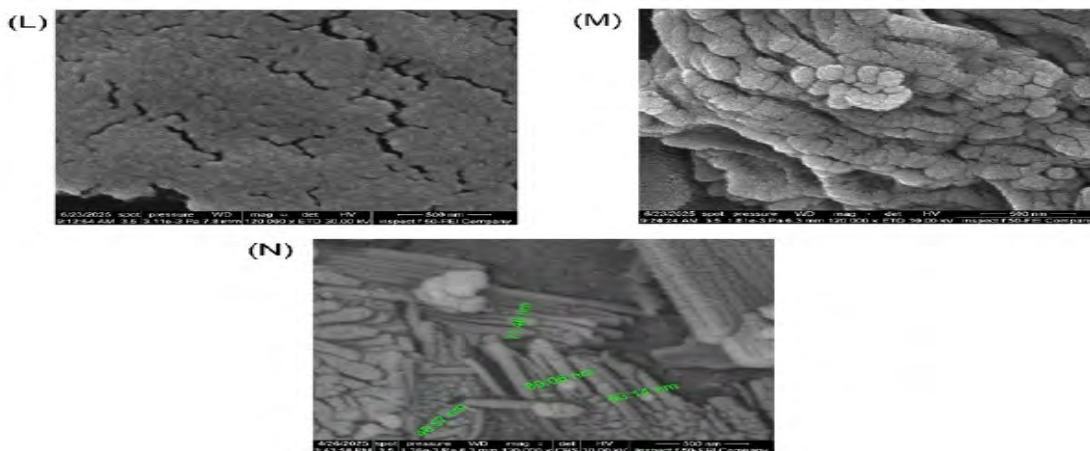


Figure 4. FESEM image (L) of chitosan, (M) of chitosan with sodium hydroxide and myrrh, (N) morphology composite chitosan-sodium hydroxide-myrrh-silver nitrate.

Biological activity

The antibacterial activity of the tested systems showed clear differences depending on composition and concentration. Chitosan alone inhibited bacterial growth at 645 ppm, which is within the commonly reported effective range and can be attributed to electrostatic interactions between its protonated amino groups and bacterial cell membranes. The chitosan–myrrh–sodium hydroxide system required a higher concentration (1940 ppm) to achieve inhibition, suggesting that alkaline treatment and interactions with myrrh partially reduced the availability of active chitosan sites, leading to reduced antibacterial efficiency. In contrast, the chitosan–myrrh–sodium hydroxide–silver nitrate composite exhibited the strongest antibacterial effect, with inhibition observed at a much lower concentration (273 ppm), highlighting the synergistic contribution of silver species in enhancing membrane damage and disrupting bacterial metabolism. Overall, the results demonstrate that silver incorporation significantly improves antibacterial performance, thereby reducing the concentration required for effective inhibition.

Conclusion

This work succeeded in synthesizing hydrogel silver nanoparticles beads infused with myrrh and silver. Incorporating myrrh and silver altered the bead structure, as shown by XRD, which revealed a decrease in the beads' crystalline nature. FESEM images revealed that the beads' surfaces were more uneven and rough after the modification, whereas FTIR analysis demonstrated that the components functioned effectively together. Additionally, the hydrogels expanded in distinct ways when exposed to acidic, neutral, and basic pH conditions. In addition, the beads demonstrated good antibacterial activity, as shown by the minimum inhibitory concentration tests. Also, decreased crystallinity and higher surface roughness show that the structure is more porous, which makes it easier for water and bacteria to enter into it. The swelling that responds to pH and the increased antibacterial activity show that chitosan, myrrh, and silver work together to make a stronger antibacterial

effect, which shows their potential for antibacterial application.

Acknowledgment

The authors would like to express their sincere gratitude to the Ministry of Higher Education and Scientific Research in Kurdistan, as well as the University of Zakho, for their invaluable support and contributions to this work.

Conflict of interest

The authors declare that they have no known competing financial interests or personal relationships that could have appeared to influence the work reported in this paper.

Funding source statement

The authors declare that they do not have received any funding.

Author contribution

Jaafar performed experimental part, wrote first draft, and revised the manuscript, and data analysis. Mohamed was supervisor of this project and revised the MS, also shared data analysis.

REFERENCES

- [1] M. Biondi, F. Ungaro, F. Quaglia, and P. A. Netti, "Controlled drug delivery in tissue engineering," *Adv. Drug Deliv. Rev.*, vol. 60, no. 2, pp. 229–242, Jan. 2008, doi: 10.1016/J.ADDR.2007.08.038.
- [2] A. Vashist, A. Vashist, Y. K. Gupta, and S. Ahmad, "Recent advances in hydrogel based drug delivery systems for the human body," *J. Mater. Chem. B*, vol. 2, no. 2, pp. 147–166, 2014, doi: 10.1039/c3tb21016b.
- [3] M. Biondi, L. Indolfi, F. Ungaro, F. Quaglia, M. I. La Rotonda, and P. A. Netti, "Bioactivated collagen-based scaffolds embedding protein-releasing biodegradable microspheres: tuning of protein release kinetics," *J. Mater. Sci. Mater. Med.*, vol. 20, pp. 2117–2128, 2009.
- [4] F. Mollica et al., "Mathematical modelling of the evolution of protein distribution within single PLGA microspheres: prediction of local concentration profiles and release kinetics," *J. Mater. Sci. Mater. Med.*, vol. 19, pp. 1587–1593, 2008.
- [5] F. Ungaro et al., "Microsphere-integrated collagen scaffolds for tissue engineering:

- Effect of microsphere formulation and scaffold properties on protein release kinetics," *J. Control. Release*, vol. 113, no. 2, pp. 128–136, Jun. 2006, doi: 10.1016/J.JCONREL.2006.04.011.
- [6] L. Mayol, M. Biondi, L. Russo, B. M. Malle, K. Schwach-Abdellaoui, and A. Borzacchiello, "Amphiphilic hyaluronic acid derivatives toward the design of micelles for the sustained delivery of hydrophobic drugs," *Carbohydr. Polym.*, vol. 102, no. 1, pp. 110–116, Feb. 2014, doi: 10.1016/J.CARBPOL.2013.11.003.
- [7] L. Mayol et al., "Injectable thermally responsive mucoadhesive gel for sustained protein delivery," *Biomacromolecules*, vol. 12, no. 1, pp. 28–33, 2011.
- [8] L. Mayol, F. Quaglia, A. Borzacchiello, L. Ambrosio, and M. I. La Rotonda, "A novel poloxamers/hyaluronic acid in situ forming hydrogel for drug delivery: Rheological, mucoadhesive and in vitro release properties," *Eur. J. Pharm. Biopharm.*, vol. 70, no. 1, pp. 199–206, 2008.
- [9] A. Borzacchiello et al., "Structural and rheological characterization of hyaluronic acid-based scaffolds for adipose tissue engineering," *Biomaterials*, vol. 28, no. 30, pp. 4399–4408, Oct. 2007, doi: 10.1016/J.BIOMATERIALS.2007.06.007.
- [10] D. Guarnieri et al., "Effects of fibronectin and laminin on structural, mechanical and transport properties of 3D collagenous network," *J. Mater. Sci. Mater. Med.*, vol. 18, pp. 245–253, 2007.
- [11] A. Maltese et al., "Novel polysaccharides-based viscoelastic formulations for ophthalmic surgery: rheological characterization," *Biomaterials*, vol. 27, no. 29, pp. 5134–5142, 2006.
- [12] B. V Slaughter, S. S. Khurshid, O. Z. Fisher, A. Khademhosseini, and N. A. Peppas, "Hydrogels in regenerative medicine," *Adv. Mater.*, vol. 21, no. 32 33, pp. 3307–3329, 2009.
- [13] A. M. Kloxin, C. J. Kloxin, C. N. Bowman, and K. S. Anseth, "Mechanical properties of cellularly responsive hydrogels and their experimental determination," *Adv. Mater.*, vol. 22, no. 31, pp. 3484–3494, 2010.
- [14] A. Borzacchiello, L. Mayol, O. Gärskog, Å. Dahlqvist, and L. Ambrosio, "Evaluation of injection augmentation treatment of hyaluronic acid based materials on rabbit vocal folds viscoelasticity," *J. Mater. Sci. Mater. Med.*, vol. 16, pp. 553–557, 2005.
- [15] A. Borzacchiello, L. Mayol, A. Schiavinato, and L. Ambrosio, "Effect of hyaluronic acid amide derivative on equine synovial fluid viscoelasticity," *J. Biomed. Mater. Res. Part A An Off. J. Soc. Biomater. Japanese Soc. Biomater. Aust. Soc. Biomater. Korean Soc. Biomater.*, vol. 92, no. 3, pp. 1162–1170, 2010.
- [16] B. T. Iber, N. A. Kasan, D. Torsabo, and J. W. Omuwa, "A review of various sources of chitin and chitosan in nature," *J. Renew. Mater.*, vol. 10, no. 4, pp. 1097–1123, 2022, doi: 10.32604/JRM.2022.018142.
- [17] J. Wang and S. Zhuang, "Chitosan-based materials: Preparation, modification and application," *J. Clean. Prod.*, vol. 355, p. 131825, 2022.
- [18] C. L. Ke, F. S. Deng, C. Y. Chuang, and C. H. Lin, "Antimicrobial actions and applications of Chitosan," *Polymers (Basel)*, vol. 13, no. 6, 2021, doi: 10.3390/polym13060904.
- [19] I. Aranaz et al., "Chitosan: An overview of its properties and applications," *Polymers (Basel)*, vol. 13, no. 19, p. 3256, 2021.
- [20] X. Che et al., "Application of Chitosan-Based Hydrogel in Promoting Wound Healing: A Review," *Polymers (Basel)*, vol. 16, no. 3, pp. 1–20, 2024, doi: 10.3390/polym16030344.
- [21] E. Rostami, "Progresses in targeted drug delivery systems using chitosan nanoparticles in cancer therapy: A mini-review," *J. Drug Deliv. Sci. Technol.*, vol. 58, p. 101813, 2020.
- [22] G. E.-S. Batiha et al., "Commiphora myrrh: a phytochemical and pharmacological update," *Naunyn. Schmiedebergs. Arch. Pharmacol.*, vol. 396, no. 3, pp. 405–420, 2023.
- [23] R. Ibrahim, "Contribution in the quality assessment of myrrh," *Rec. Pharm. Biomed. Sci.*, vol. 8, no. 2, pp. 46–64, 2024.
- [24] M.-S. Yang et al., "Antiviral and therapeutic effects of a mixture of *Boswellia serrata*, *Commiphora myrrh*, and Propolis for SARS-CoV-2," *Nat. Prod. Commun.*, vol. 18, no. 7, p. 1934578X231180709, 2023.
- [25] K. S. Siddiqi, A. Husen, and R. A. K. Rao, "A review on biosynthesis of silver nanoparticles and their biocidal properties," *J. Nanobiotechnology*, vol. 16, no. 1, p. 14,

- 2018.
- [26] C. Marambio-Jones and E. M. V. Hoek, "A review of the antibacterial effects of silver nanomaterials and potential implications for human health and the environment," *J. Nanoparticle Res.*, vol. 12, no. 5, pp. 1531–1551, 2010.
- [27] R. A. Mauricio-Sánchez, R. Salazar, J. G. Luna-Bárcenas, and A. Mendoza-Galván, "FTIR spectroscopy studies on the spontaneous neutralization of chitosan acetate films by moisture conditioning," *Vib. Spectrosc.*, vol.